

Coupled plasmon–LOphonon modes in GaInAs quantum wires

N. Mutluay and B. Tanatar

Citation: *J. Appl. Phys.* **80**, 4484 (1996); doi: 10.1063/1.363427

View online: <http://dx.doi.org/10.1063/1.363427>

View Table of Contents: <http://jap.aip.org/resource/1/JAPIAU/v80/i8>

Published by the [American Institute of Physics](#).

Additional information on J. Appl. Phys.

Journal Homepage: <http://jap.aip.org/>

Journal Information: http://jap.aip.org/about/about_the_journal

Top downloads: http://jap.aip.org/features/most_downloaded

Information for Authors: <http://jap.aip.org/authors>

ADVERTISEMENT



AIPAdvances

Now Indexed in
Thomson Reuters
Databases

Explore AIP's open access journal:

- Rapid publication
- Article-level metrics
- Post-publication rating and commenting

Coupled plasmon–LO-phonon modes in GaInAs quantum wires

N. Mutluay and B. Tanatar^{a)}

Department of Physics, Bilkent University, Bilkent, 06533 Ankara, Turkey

(Received 16 April 1996; accepted for publication 20 June 1996)

We study the collective excitation modes of coupled quasi-one-dimensional electron gas and longitudinal-optical phonons in GaInAs quantum wires within the random-phase approximation. In contrast to the higher-dimensional systems, the plasmon–phonon coupling is found to be strong at all linear carrier densities of interest. We calculate the oscillator strength of the numerically evaluated coupled modes and the Raman scattering intensity. The effect of phenomenological LO-phonon broadening on the collective excitation spectrum is also investigated. © 1996 American Institute of Physics. [S0021-8979(96)02019-1]

I. INTRODUCTION

In a degenerate polar semiconductor, such as n -type GaAs, the longitudinal optical (LO) phonons of the underlying lattice couple to the free carriers in the system. Macroscopically, the electric dipole moment associated with LO phonons couples with the electric field of the collective charge oscillations (plasmons). On a microscopic level the electron–LO-phonon interaction results in a many-body renormalization of the collective modes as well as various other single-particle properties of the free carriers. The coupled collective excitations in doped semiconductors are experimentally probed by such methods as Raman scattering, energy-loss spectroscopy, and transport measurements. The plasmon–phonon coupling in GaAs has been studied extensively by Raman scattering.¹ The ternary compound GaInAs, on the other hand, is a two-mode system and has been found suitable for electronic device applications such as high electron mobility transistors, heterojunction bipolar transistors, and for optoelectronic applications like photodetectors and lasers.² A vast amount of research activity^{3–6} on this and related materials reflects the potential in such possibilities.

In this work, we study the coupled plasmon–LO-phonon modes of a GaInAs-based quantum wire system within the random-phase approximation (RPA). The main motivation is to explore the interplay between the quasi-one-dimensional (Q1D) character of the charge carriers and the various phonon modes in the system, which is expected to yield a strong mode coupling. Q1D electron systems as they occur in semiconducting structures are based on the carrier confinement in transverse directions, causing the electrons to move freely in one space direction. The chief motivation for studying these low-dimensional systems comes from their technological potential such as high-speed electronic devices and quantum-wire lasers. Work on coupled plasmon–phonon modes in Q1D GaAs systems has revealed many interesting properties.⁷ Specifically, GaInAs quantum wires are beginning to be manufactured.⁸ Other than the practical implications, electrons in Q1D structures offer an interesting many-body system for condensed-matter theories.

The rest of this article is organized as follows. In Sec. II we outline the model of a quantum-wire structure and the

calculation of coupled plasmon-phonon modes in GaInAs. Our results for the dispersion and spectral properties of the collective excitations are provided in Sec. III. We conclude with a brief summary.

II. PLASMON–PHONON COUPLING

We calculate the total longitudinal dielectric function $\varepsilon_T(q, \omega)$ of the Q1D electron gas at zero temperature in a polar semiconductor with two LO-phonon modes. The collective modes of the system will be given by the poles of $\text{Re}[\varepsilon_T(q, \omega)] = 0$, in the region where $\text{Im}[\varepsilon_T(q, \omega)] = 0$. Within the (RPA) the polarizabilities of the phonon and electron subsystems are additive and we express the total dielectric function as

$$\varepsilon_T(q, \omega) = \varepsilon_{\text{ph}}(\omega) - V(q)\chi_0(q, \omega),$$

where $\varepsilon_{\text{ph}}(\omega)$ is the phonon part of the dielectric function, $V(q)$ is the Coulomb interaction between the electrons, and $\chi_0(q, \omega)$ is the complex dynamic susceptibility for the non-interacting system.⁹ Note that we do not make the large frequency approximation to $\chi_0(q, \omega)$. Using bulk, dispersionless phonon modes the phonon part ε_{ph} is given by^{10,11}

$$\varepsilon_{\text{ph}}(\omega) = 1 - \frac{\omega_{\text{TO}}^2 - \omega_{\text{LO}}^2}{\omega_{\text{TO}}^2 - \omega^2 - i\gamma\omega} - \frac{\omega_{\text{LO}}^2}{\omega_{\text{TO}}^2} \frac{\omega_{\text{TO}'}^2 - \omega_{\text{LO}'}^2}{\omega_{\text{TO}'}^2 - \omega^2 - i\gamma\omega}. \quad (1)$$

In the above, ω_{LO} and ω_{TO} denote the InAs-like phonon modes, whereas $\omega_{\text{LO}'}$ and $\omega_{\text{TO}'}$ denote the GaAs-like phonon modes. We have also added a phenomenological phonon damping term characterized by γ . Letting $\gamma \rightarrow 0$ renders $\varepsilon_{\text{ph}}(\omega)$ purely real.

For the Q1D electron gas, we consider a cylindrical wire with radius R and infinite potential barriers.¹² The electrons are embedded in a uniform positive background to maintain charge neutrality. We treat the electron system as a Fermi liquid, i.e., with a well-defined Fermi surface at zero temperature and interaction via Coulomb potential,¹³ which seems to be supported by the experimental observations¹⁴ of collective excitations in GaAs quantum wires. The linear electron density N in the wire is related to the Fermi wave vector by $N = 2k_F / \pi$. We also define the dimensionless electron gas parameter $r_s = \pi / (4k_F a_B^*)$, in which $a_B^* = \epsilon_\infty / (e^2 m^*)$ is the effective Bohr radius in the semicon-

^{a)}Electronic mail: tanatar@fen.bilkent.edu.tr

ducting wire with high-frequency dielectric constant ϵ_∞ and electron effective mass m^* . The Coulomb interaction potential in the quantum wire system is given by¹²

$$V(q) = \frac{e^2}{\epsilon_\infty} \frac{72}{(qR)^2} \left[\frac{1}{10} - \frac{2}{3(qR)^2} + \frac{32}{3(qR)^4} - 64 \frac{I_3(qR)K_3(qR)}{(qR)^4} \right], \quad (2)$$

where $I_n(x)$ and $K_n(x)$ are modified Bessel functions. We note that the choice of a cylindrical geometry is largely immaterial since the obtained results are qualitatively similar to those using different quantum wire models.⁷ For more realistic structures self-consistent calculations could be employed to determine the Coulomb potential.¹⁵ We assume that only the lowest subband in the quantum wire is occupied. This will hold as long as the difference between the second and first subbands, Δ_{21} remains much larger than the temperature T (we take Boltzmann constant $k_B = 1$).

The collective charge excitations of an uncoupled quantum wire system (electronic part only) at zero temperature is given by $\epsilon[q, \omega_{\text{pl}}(q)] = 0$. At $T = 0$, one obtains¹⁶

$$\omega_{\text{pl}}^2(q) = \frac{\omega_+^2 e^{F(q)} - \omega_-^2}{e^{F(q)} - 1}, \quad (3)$$

where $\omega_\pm = |q^2/2m^* \pm qk_F/m^*|$, and $F(q) = (\pi q/m^*)/V(q)$. The long-wavelength limit of the plasmon dispersions (in the RPA) are given by^{12,16}

$$\frac{\omega_{\text{pl}}(q)}{E_F} = \frac{8}{\pi} r_s^{1/2} \frac{q}{k_F} \left[\ln \left(\frac{2}{q^2 R} \right) \right]^{1/2}, \quad (4)$$

where $r_s = 1/(2Na_B^*)$ is the electron gas parameter. The above result follows from the high-frequency expansion of the 1D polarizability and small q limit of the Coulomb potential.

III. NUMERICAL RESULTS AND DISCUSSION

We evaluate the coupled plasmon–LO-phonon modes in the GaInAs quantum wire system by solving for the zeros of $\text{Re}[\epsilon_T(q, \Omega_q)] = 0$. Specializing to the compound $\text{Ga}_x\text{In}_{1-x}\text{As}$ where $x = 0.47$, we use the values $\omega_{\text{LO}} = 233 \text{ cm}^{-1}$ and $\omega_{\text{TO}} = 226 \text{ cm}^{-1}$ for the InAs-like LO and TO modes, and $\omega_{\text{LO}'} = 272 \text{ cm}^{-1}$ and $\omega_{\text{TO}'} = 256 \text{ cm}^{-1}$ for the GaAs-like LO and TO modes, respectively.^{10,11} The effective mass of electrons is taken to be $m^* = 0.047m_e$. Altogether we find four modes: $\Omega_q^{(1)}$ and $\Omega_q^{(2)}$ refer to the GaAs and InAs-like coupled modes, whereas $\Omega_q^{(3)}$ and $\Omega_q^{(4)}$ are coupled plasmon modes. Figure 1 shows the calculated coupled and uncoupled modes for the linear carrier densities $N = 5 \times 10^5 \text{ cm}^{-1}$ [Fig. 1(a)] and $N = 10^6 \text{ cm}^{-1}$ [Fig. 1(b)] in a quantum wire with radius $R = 100 \text{ \AA}$. The LO-phonon modes and plasmon excitations for the coupled system are shown by the solid lines. We find that the GaAs-like coupled phonon mode starts off at a slightly higher energy than the uncoupled $\omega_{\text{LO}'}$, which is indicated by the topmost horizontal dashed line. The InAs-like phonon mode, on the other hand, is slightly lowered in energy for small q values compared to ω_{LO} . Both coupled phonon modes increase with increasing

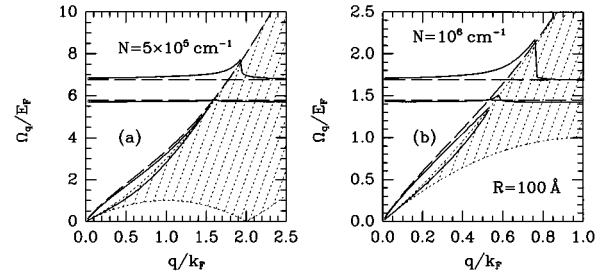


FIG. 1. The dispersion of coupled (solid lines) and uncoupled (dashed lines) plasmon–phonon modes in GaInAs quantum wire with radius $R = 100 \text{ \AA}$, and for carrier densities (a) $N = 5 \times 10^5 \text{ cm}^{-1}$ and (b) $N = 10^6 \text{ cm}^{-1}$. The region bounded by the dotted lines shows the particle–hole continuum for a 1D system.

q until they reach the particle-hole (p–h) continuum defined by the shaded area, after which they are Landau damped and their energy decreases. We also note that the coupled phonon modes never cross the respective TO-phonon frequencies. In Fig. 1 the low-energy excitations (shown by the solid lines) belong to the coupled plasmons. For comparison the uncoupled plasmon mode^{12,16} is indicated by the dashed line and it asymptotically approaches the upper boundary of the particle–hole excitation region. For the uncoupled system, this mode becomes the one that lies outside the p–h continuum. For small q ,

$$\Omega_q^{(3)} \sim (\omega_{\text{TO}}/\omega_{\text{LO}})(\omega_{\text{TO}'}/\omega_{\text{LO}'})\omega_{\text{pl}}(q),$$

where the uncoupled plasmon mode $\omega_{\text{pl}}(q)$ is given in Eq. (4). It undergoes Landau damping at a critical wave vector q_c [$q_c \approx 1.5k_F$ and $0.5k_F$ in Figs. 1(a) and 1(b)], respectively) as it enters the p–h continuum. It is evident from Figs. 1(a) and 1(b) that mode coupling is strong at both densities and at wave vectors away from the resonance where the uncoupled plasmon mode equals ω_{LO} or $\omega_{\text{LO}'}$. Such a strong 1D plasmon–phonon coupling is a consequence of the logarithmic singularity in the 1D polarizability,⁹ which makes it possible for the uncoupled plasmon mode to exist for all wave vectors. The other plasmon mode which lies inside the p–h region is heavily damped for all wave vectors. This led Hwang and Das Sarma⁷ (in a different but related context) to coin $\Omega_q^{(3)}$ to be the true coupled plasmon mode, and to dismiss $\Omega_q^{(4)}$ altogether on the grounds that it would be unobservable. In general, the wave vector dependence of the collective excitations we obtain is qualitatively similar to that found¹¹ for GaInAs heterostructures.

In order to better assess the relative importance of the collective modes in a GaInAs quantum wire system, we calculate the oscillator strength given by

$$A(q) = \pi \left(\frac{\partial}{\partial \omega} \text{Re} \left[\epsilon_T(q, \omega) \right] \Big|_{\Omega_q} \right)^{-1}. \quad (5)$$

In Figs. 2(a) and 2(b) we show the oscillator strength $A(q)$ for densities $N = 5 \times 10^5 \text{ cm}^{-1}$ and $N = 10^6 \text{ cm}^{-1}$, respectively. We observe that for all wave vectors most of the weight is carried by the GaAs-like LO-phonon mode ($\Omega_q^{(1)}$, denoted by the dashed line) where its weight gradually increases until it enters the p–h region. The InAs-like

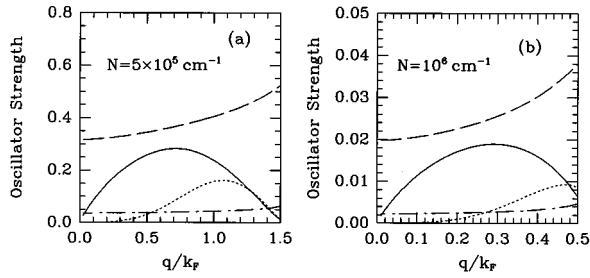


FIG. 2. The oscillator strength $A(q)$, of coupled modes for (a) $N = 5 \times 10^6 \text{ cm}^{-1}$ and (b) $N = 10^6 \text{ cm}^{-1}$. The solid and dotted lines indicate the true and heavily damped plasmon modes, whereas the dashed and dotted-dashed lines indicate the GaAs- and InAs-like coupled modes, respectively.

coupled mode ($\Omega_q^{(2)}$) is represented by the dotted-dashed line and it carries a relatively smaller weight. That the InAs-like mode is very weak has been observed in *p*-type GaInAs samples.⁵ The solid line shows the oscillator strength for the true plasmon mode $\Omega_q^{(3)}$ which vanishes as the mode enters the Landau damping region. The second plasmon mode $\Omega_q^{(4)}$ which is heavily damped is denoted by the dotted line, and it has the smallest weight.

The dynamic structure factor $S(q, \omega)$, which gives the spectral weight of the collective modes and single-particle excitations, is a central quantity¹⁷ in light-scattering experiments. The various peaks in $S(q, \omega)$ are associated with the collective excitation energies. $S(q, \omega)$ is proportional to the imaginary part of the inverse dielectric function, and in Fig. 3 we display $\text{Im}[\epsilon_T^{-1}(q, \omega)]$ as a function of ω for $N = 10^6 \text{ cm}^{-1}$ and $R = 100 \text{ \AA}$. We expect to see peaks corresponding to the coupled phonon and plasmon modes, as well as the contribution from the single-particle excitation region. As the previous oscillator strength analysis reveals the heavily damped second plasmon mode $\Omega_q^{(4)}$ should not show any significant weight. In Fig. 3 curves from bottom to top indicate $q/k_F = 0.2, 0.4, 0.6, 0.7,$ and 0.8 , respectively. As the wave vector q is increased the low-energy peak which is the contribution from the single-particle excitations moves toward higher energies and its width broadens. The δ -function peaks of the collective excitations are indicated by arrows.

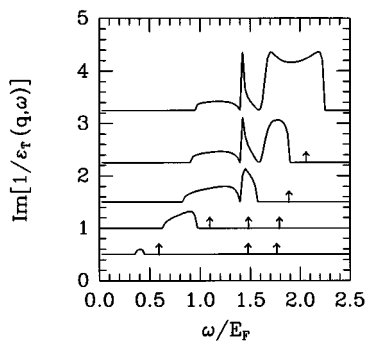


FIG. 3. The electron energy-loss function as a function of frequency for different values of the wave vector q . From bottom to top, $q/k_F = 0.2, 0.4, 0.6, 0.7,$ and 0.8 . The arrows indicate the undamped collective excitations which appear as δ -function peaks.

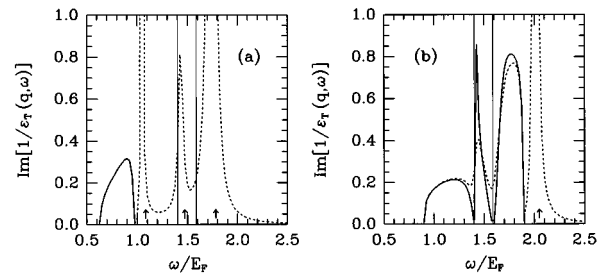


FIG. 4. The electron energy-loss function $\text{Im}[\epsilon_T^{-1}(q, \omega)]$ for $N = 10^6 \text{ cm}^{-1}$ GaInAs quantum wire at (a) $q = 0.4k_F$ and (b) $q = 0.7k_F$. The dotted and solid lines represent the scattering intensity with and without the phenomenological phonon broadening, respectively, taken as $\gamma = 0.05E_F$. Vertical thin lines show the TO-phonon frequencies. The locations of nonbroadened collective modes are indicated by small arrows.

The influence of a finite relaxation time for the unperturbed phonon modes on the energy-loss function is depicted in Fig. 4 for (a) $q = 0.4k_F$ and (b) $q = 0.7k_F$, for $N = 10^6 \text{ cm}^{-1}$. The solid curve corresponds to the result without broadening and the dotted curve is the energy-loss spectrum in the presence of phonon broadening with a typical value of $\gamma = 0.05E_F$. The spectrum is not appreciably altered for the single-particle excitation region (broad low-energy peak) but the sharp LO-phonon modes are smoothed. The locations of the collective modes in the absence of phonon broadening are indicated by arrows of which the spectral weights may be read off from Fig. 2. Furthermore, at the TO-phonon frequencies (indicated by thin vertical lines) the spectrum attains finite values because of the broadening.

The frequency of the collective excitations are often measured as a function of the electron density N at a fixed wave vector. Since the long-wavelength limit is most easily accessible experimentally, we choose $q = 0.2k_F$ to show the density dependence of the coupled modes in Fig. 5. The top two curves represent the $\Omega_q^{(1)}$ and $\Omega_q^{(2)}$, respectively, and the bottom curve the coupled plasmon mode $\Omega_q^{(3)}$. For comparison the uncoupled LO-phonon modes and the plasmon mode are also shown by the dashed lines. There are several noteworthy features. The frequency of the InAs-like coupled mode varies very little with the linear carrier density. The GaAs-like mode exhibits a peak around $N \approx 2.4 \times 10^6$

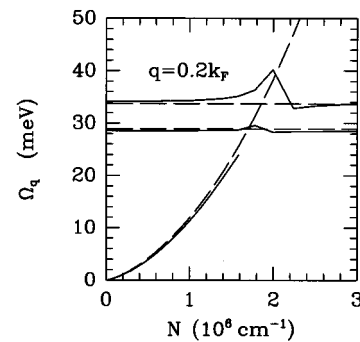


FIG. 5. The dispersion of the collective excitations as a function of the carrier density N at $q = 0.2k_F$. The thick lines, from top to bottom, indicate the coupled modes $\Omega_q^{(1)}$, $\Omega_q^{(2)}$, and $\Omega_q^{(3)}$, respectively, whereas the dashed lines show the corresponding uncoupled modes.

cm^{-1} . Although the uncoupled plasmon mode seems to exist for all densities, the coupled plasmon mode ceases to exist for $N > 1.6 \times 10^6 \text{ cm}^{-1}$. This critical density corresponds to the value of $\Omega_q^{(3)}$ where it approaches the uncoupled InAs TO-phonon frequency.

We now remark on some aspects of the present work. We have based our mode-coupling analysis in Q1D electron systems on the RPA. For the densities of experimental interest, $N \sim 10^5 - 10^6 \text{ cm}^{-1}$ ($r_s \sim 1 - 5$), this mean-field approximation should be valid. The reason for the remarkable applicability of the RPA is attributed to the limited phase space in Q1D systems compared to higher dimensions.^{7,13} In GaAs-based quantum wires, measured collective excitations are readily interpreted within the RPA.¹⁴ Although our calculations for the dispersion relations and Raman scattering intensities of coupled plasmon-phonon modes were for an n -type GaInAs, similar analysis can be made for a p -type GaInAs where, owing to the larger effective mass of holes, plasmon damping effects are expected to be important.⁵ It would also be possible to calculate the inelastic scattering rate^{7,13} of electrons $\Gamma_q = |\text{Im} \Sigma(q, \epsilon_q)|$, for the Q1D GaInAs quantum wire using our results for the dielectric function in the self-energy expression $\Sigma(q, \omega)$. In this work we have considered the coupling between Q1D electrons and bulk phonon modes only. The interface phonon modes are likely to change the coupled mode excitations discussed here, in particular at smaller wire radii $R \sim 50 \text{ \AA}$. The phonon part of the dielectric function ϵ_{ph} in the presence of interface phonon modes with dispersion would then need to be modified using standard techniques.¹⁷

In summary, we have investigated the coupled plasmon-phonon modes in a GaInAs quantum wire system within the RPA at zero temperature. We have calculated the dispersion and spectral weight of the coupled collective excitations. Similar to the GaAs quantum wires, we found the mode-coupling effect to be strong at all densities and wave vectors of practical interest in contrast to the corresponding higher-dimensional cases.

ACKNOWLEDGMENTS

This work is partially supported by the Scientific and Technical Research Council of Turkey (TUBITAK) under Grant No. TBAG-AY/77. We thank Dr. N. Balkan and C. R. Bennett for useful discussions.

- ¹D. Olego and M. Cardona, *Phys. Rev. B* **24**, 7217 (1981); G. Irmer, V. V. Toporov, B. H. Bairamov, and J. Monecke, *Phys. Status Solidi B* **119**, 595 (1983); K. Wan, J. F. Young, R. L. S. Devine, W. T. Moore, A. J. S. Thorpe, C. J. Miner, and P. Mandeville, *J. Appl. Phys.* **63**, 5598 (1988).
- ²S. D. Gunapala, B. F. Levine, D. Ritter, R. Hamm, and M. B. Panish, *Appl. Phys. Lett.* **48**, 2024 (1991); J. H. March, J. S. Roberts, and P. A. Claxton, *ibid.* **46**, 1161 (1985).
- ³A. J. Vickers and L. Kapetanakis, *Semicond. Sci. Technol.* **10**, 829 (1995); K. Häusler, K. Eberl, and W. Sigle, *ibid.* **10**, 167 (1995).
- ⁴T. W. Kim, M. Jung, D. U. Lee, and K. H. Yoo, *Semicond. Sci. Technol.* **10**, 84 (1995); M. Fritze, A. V. Nurmikko, and P. Hawrylak, *Phys. Rev. B* **48**, 4960 (1993).
- ⁵M. Qi, M. Konagai, and K. Takahashi, *J. Appl. Phys.* **78**, 7265 (1995).
- ⁶D. Ahn, *J. Appl. Phys.* **78**, 4505 (1995).
- ⁷E. H. Hwang and S. Das Sarma, *Phys. Rev. B* **52**, R8668 (1995); L. Wendler, R. Haupt, and R. Pechstedt, *Phys. Rev. B* **43**, 14669 (1991); *Surf. Sci.* **263**, 363 (1992).
- ⁸J. Wagner, D. Behr, D. Richards, T. Bickl, A. Forchel, M. Emmerling, and K. Köhler, *Superlattices and Microstructures* **14**, 265 (1993); R. Steffen, Th. Koch, J. Oshinowo, F. Faller, and A. Forchel, *Appl. Phys. Lett.* **68**, 223 (1996).
- ⁹P. F. Williams and A. N. Bloch, *Phys. Rev. B* **10**, 1097 (1974).
- ¹⁰J. C. Portal, G. Gregoris, M. A. Brummell, R. J. Nicholas, M. Razeghi, M. A. Di Forte-Poisson, K. Y. Cheng, and A. Y. Cho, *Surf. Sci.* **142**, 368 (1984).
- ¹¹F. M. Peeters, X. Wu, and J. T. Devreese, *Phys. Rev. B* **36**, 7518 (1987).
- ¹²A. Gold and A. Ghazali, *Phys. Rev. B* **41**, 7626 (1990).
- ¹³B. Y.-K. Hu and S. Das Sarma, *Phys. Rev. B* **48**, 14 388 (1993).
- ¹⁴A. R. Goñi, A. Pinczuk, J. S. Weiner, J. M. Calleja, B. S. Dennis, L. N. Pfeiffer, and K. W. West, *Phys. Rev. Lett.* **67**, 3298 (1991); A. Schmeller, A. R. Goñi, A. Pinczuk, J. S. Reiner, J. M. Calleja, B. S. Dennis, L. N. Pfeiffer, and K. W. West, *Phys. Rev. B* **49**, 14 778 (1994).
- ¹⁵S. E. Laux and F. Stern, *Appl. Phys. Lett.* **49**, 91 (1986).
- ¹⁶Q. P. Li and S. Das Sarma, *Phys. Rev. B* **43**, 11 768 (1991).
- ¹⁷D. Pines and P. Nozieres, *The Theory of Quantum Liquids* (W. A. Benjamin, New York, 1966); G. D. Mahan, *Many Particle Physics* (Plenum, New York, 1981).